*DOI:*
10.1109/TVT.2019.2917426

*Document Version*
Peer reviewed version

1

# Inter-Tenant Resource Sharing and Power Allocation in 5G Virtual Networks

Jinwei Gang, Student Member, IEEE and Vasilis Friderikos, Member, IEEE

***Abstract*—Recently the concept of network virtualization and network slicing attracted significant attention from both industry and academia as a key component of the evolving 5G architecture to allow the efficient entrance of vertical industries and tackle increased aggregate traffic by flexible network re-configurability. However, the potential price to be paid for facilitating network slicing in a multi-tenant virtual network is the underutilization of the scarce wireless network resources due to the different tenant requirements and the inherent dynamics of the traffic. A potential way to avoid such sacrifice of radio resources is to allow efficient inter-tenant resource sharing. To this end, this work proposes a novel optimization framework for flexible inter-tenant resource sharing embedded with transmission power control to aggressively improve network capacity, the utilization of wireless access resources, user data rate as well as energy efficiency. More specifically, we define two novel resource sharing mechanisms called Tight Coupling (TX) and Loose Coupling (LX), respectively, via Mixed Integer Linear Programming (MILP) formulations. Furthermore, two Resource and Power Joint Allocation (RPJA) algorithms are designed to solve the optimization problem in polynomial time. Based on 3GPP network parameterization, a rigorous analysis via a wide set of numerical investigations reveal that significant gains in network throughput, individual user rate and energy efficiency, can be achieved compared with current baseline network slicing methods and constant power resource sharing algorithms.**

***Index Terms*—5G networks, mathematical programming, network virtualization, resource sharing, resource reuse, optimization, energy efficiency.**

## I. Introduction

OVER the last few years, significant attention has been placed on defining and architecturing 5G communication networks; a central focus on the design is to enable significant levels of programmability and flexibility in addition to advanced schemes that will allow denser deployment of heterogeneous networks (HetNets) [1]. These emerging networks are expected to provide highly increased data rates but more importantly to efficiently and cost-effectively support new services and vertical market integration to create in that sense an integrated ecosystem for both technical as well as business innovation [2]. However, the densely deployed multi-tier networks that combining both macro base station (MBS) and small base station (SBS) can cause significant operating cost in infrastructure and cumbersome network management/cooperation. On this point, enabling the logically isolated, coexisted and shareable virtual networks within the physical substrate infrastructure is considered as a fundamental component of future 5G networks [3]. In terms of wireless resources, resource slicing and potential sharing among multi-service provider (SP)/tenants[1] is the key to support the envisioned diversity and increased overall capacity in the networks. By combining these concepts and technologies, the costs reduction of infrastructure provider (InP) (both CAPEX and OPEX), and efficient cooperation between SPs can be achieved.

Hand in hand with the aforementioned techniques and benefits, a set of challenges also arrive when bringing virtualization functionalities to a dense multi-tier Radio Access Network (RAN). Although the Third-Generation Partnership Project (3GPP) [4] has standardized certain functionalities to motivate multiple SPs to share a cellular network, there are still limitations in the definition of the specific resource assignment techniques among virtual slices and the detailed implementation of functionalities. Summarized in articles [3]-[6], open-ended research aspects are in the following areas: (1) how wireless network resources be shared and reused efficiently between tenants based on customized tenancy agreements, (2) how wireless resources be allocated dynamically and flexibly in virtual network with varying traffic demand (especially in overloaded network scenarios) and finally (3) how the increased traffic control signalling that occurs due to the communication between SPs and InPs be handled to ensure an efficient and robust operation of the network. In the view of wireless architecture, these issues become more challenging when applying multi-tier HetNets in which overlapped and densely deployed base stations, where strong co-channel interference emerges, need to be controlled.

To this end, by studying the present state of the art and principle of network architecture, we hereby propose an optimization framework to flexibly share and reuse the OFDMA (Orthogonal Frequency Division Multiple Access) based physical resource block (PRB) among tenants in a virtualized wireless network. Furthermore, to aggressively improve the overall network capacity and avoid overwhelming levels of interference, we combine the proposed resource reuse approach with transmission power control and shed further light on different degrees of resource sharing. More specifically, this work defines a resource reuse maximization problem in form of a MILP, and provides two low complexity algorithms to achieve tangible improvement in system throughput, per user achievable rate and energy efficiency. We note that the proposed schemes are inline with emerging network architecture concepts in Software Defined Network (SDN) such as C/U split (Control plane/User plane split) network [7] or the so-called 'super base station' [8] that provide the overarching

Manuscript

[1]In this paper the terms SP and tenant are used interchangeably.

framework to limit control plane signalling in the network and inter-tier interference.

### A. State of The Art and Related Works

With the tremendous growth in mobile network traffic and the need to accommodate new vertical markets in the mobile/wireless ecosystem, the role of network virtualization to RAN is becoming enormously significant [9]. The mobile carrier networks in this case have to satisfy two main requirements: coexistence and isolation of multiple virtual networks [3][10][11]. In terms of wireless resources, network slicing is a more specific concept to realize a virtual network, which is usually defined as the assignment of a subset of network resources or functionalities to certain tenants for supporting their end users [12]. Summarized in [3], network slicing can be considered in three levels: spectrum, infrastructure and network. To realize efficient network slicing and reliable virtualization services, SDN bound with network function virtualization (NFV) is seen as the key enabler for future 5G networks. The main principle of SDN is to decouple the data forwarding and control planes of a network, motivating in that respect a flexible and simplified network management [13][14]. The centralized control plane normally can be located in a data center of the core network/central cloud [15]; however, with the trend of denser cell deployment in HetNets, the control plane is also considered to be located in the cloud edge or even decentralized at the MBS. As proposed in [7][8], if the control plane is implemented in a MBS (like a C/U split or the so-called 'super BS' architecture), such MBS is able to manage the whole system resources horizontally and guide SBS or RRH (remote radio head) to assign virtual resources to users without cross tier interference. In this work, the C/U split architecture is considered as the foundation architectural element to embed the proposed optimization framework and algorithms. On the other hand, NFV assists SDN by providing management/cooperation within network entities without hardware restriction as in traditional networks [16]. The Cloud-RAN proposed by Chen and Hadzialic *et al* [17][18] shows an example of taking signal processing functions from physical base station to the cloud. Similarly, authors in [19] illustrates NFV of the Evolved Packet Core (EPC), a core network with different functional entities, in LTE networks. In their work, the virtualized functions of all entities are stored in the cloud in the sense of a Cloud-RAN.

Based on the present state of the art, solutions dedicated to perform intelligent slicing and virtual resources assignment are widely studied. The authors in [10] provide a detailed comparison between different sharing approaches that could be applied to current or emerging wireless architectures. In order to motivate flexibility in traditional static resource reservation (SR)/fixed slicing, a well-known concept named network virtualization substrate (NVS) is proposed [20] and further enhanced in [21], [22], [23]. The NVS scheme specifies two approaches of resource slicing with customized scheduling techniques. These two approaches are named as bandwidth based NVS and resource based NVS, indicating resource slicing based on application/service bandwidth requirement or amount of aggregated resources required by a tenant, respectively. Unfortunately, these approaches only consider single cell scenarios. Considering a multi-tier network with dense cell deployment, work in [24] presents an optimization scheme to jointly allocate power and subchannel resources in a two-tier network with functional virtualization. Similarly, a 5G network based control plane is proposed by [25] to perform trade-off between resource slicing and user mobility. Moreover, authors in [26][27] introduce a set of game theory based methods to dynamically assign system bandwidth as an auction game in virtualized wireless networks. However, underutilization of resources and infeasibility to cope with dynamic traffic are still the issues once customized resource assignment and slicing is done by the methods mentioned above. Thus, we further research several proposals that could be used to solve the issues. We found that works in [28] and [29] present two different methods to re-assign radio resources between slices in a short time basis. Meanwhile, authors in [23] also propose a novel version of NVS with the so called PRR (partial resource reservation) technique defining certain 'mutual resources' reserved in the network to compensate unbalanced traffic between tenants in time.

### B. Contributions and Structure

Based on the current state of the art and related works, and to the best of our knowledge there is no previous work that enables different levels of resource reuse of orthogonal resources by introducing scalable degrees of inter-tenant sharing with controllable interference in emerging 5G network architectures. As being an extension of our previous work [30], the main contributions of this work include (1) proposal of an optimization framework that offers inter-tenant resource reuse/allocation with different sharing flexibility and operation complexity (LX and TX) in a virtual wireless network environment, (2) an illustration of practical implementation of the proposed scheme in an SDN network enabled by specified software defined mobile controller (SDM) [31], (3) an investigation on binding variable transmission power to motivate further inter-tenant resource reuse with benefit of improved energy efficiency, and (4) two heuristic based algorithms (RPJA-h and RPJA-adv) that can be embedded in network controllers to provide efficient sub-optimal solutions to the optimization problem. In this paper we provide a deterministic optimization framework using integer linear programming. In that setting the salient assumption is that batch processing of the requests is performed; for example this can be done by introducing a small delaying and process a number of requests together. Another way on looking at this problem is to assume some form of knowledge regarding future requests and perform stochastic optimization [47]. In that case, since our proposed framework assumes perfect knowledge we can consider it as providing a bound on the achievable performance.

The rest of the paper is organized as follows: Section II presents the ETSI framework of SDN and NFV, where our proposed scheme and algorithms can be applied, and detailed implementation of two resource sharing mechanisms on SDM controllers. In Section III, a realistic network topology used

by the framework is introduced and the optimization problem is formulated accordingly. Section IV introduces the proposed algorithms to tackle computational complexity issues. Section V illustrates the details of the numerical investigations by comparing the proposed scheme with classic methods and Section VI concludes the work.

## II. Inter-Tenant Resource Sharing and Power Allocation Framework (LX & TX)

### A. SDN and NFV with Resource Sharing

Broadly speaking, ETSI NFV provides a very precise architectural framework for managing and orchestrating virtualized resources that relate to network functions as well services of an operator. SDN, on the other hand, can be deemed as a more generic framework compared to NFV and in that respect an ETSI NFV architecture can utilize the services of SDN to provide a programmable platform for establishing links between the various VNFs in the sense of routing and overall policy based management. At the moment, ETSI NFV is in the process of specifying the interfaces for allowing interworking between SDN controllers with the NFV MANO system, and various options have already been previously defined [32].

A number of recent EU-funded research projects like 5G NORMA further the MANO/SDN integration by leveraging on the SDN and NFV concepts to develop a novel mobile network architecture that shall provide the necessary adaptability in a resource efficient way able to handle variations in traffic demand. More specifically, 5G NORMA extends the NFV MANO framework to support multi-tenancy; a critical enabler of resource sharing. Together with that two SDN-based controllers have been defined, one for the management of network functions local to a mobile network service slice (the so-called SDM-C), and the second for the management of network functions that are common/shared between mobile network service slices (the so-called SDM-X). As can be seen in Fig.1, these controllers can be implemented as VNFs themselves since the MANO architecture supported by SDN allows for such flexibility (and in fact that was the preferred architectural decision within the project).

The proposed techniques detailed hereafter assume the existence of such flexibility on the mobile network. However the proposed set of techniques are generic enough to allow implementation in other potential architectures that support resource sharing in emerging 5G networks.

The SDM controller is usually defined in four aspects: topology, resource, function and deployment [31]. In the resource aspect, the main function SDM provides is to slice the bandwidth of the virtual network (also called SDM orchestrator in this case) and realize real-time scheduling and resource management for different network slices. To motivate high flexibility in resource management, the 5GNORMA [31] proposes a pair of distinguished SDM controllers: SDM-C and SDM-X. The details of implementation of these SDM controllers and examples of network level Demo can be found in [33]. In definition, SDM-C refers to the general controller operating in the dedicated control layer, which provides per

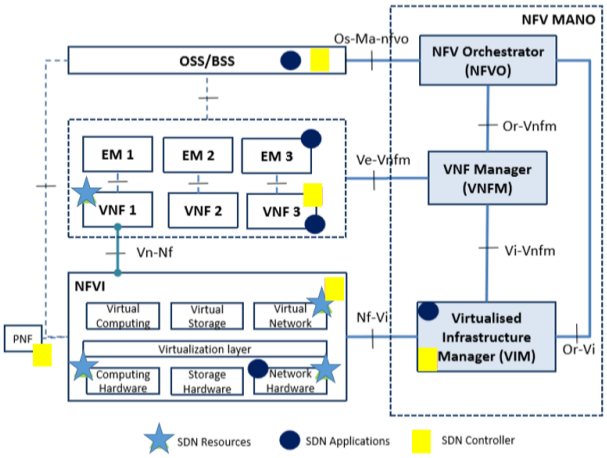


Fig. 1: Set of options of locating SDN Resources, SDN Controllers (such as SDM-C/X) and SDN Applications in the MANO NFV Architectural Framework [32].

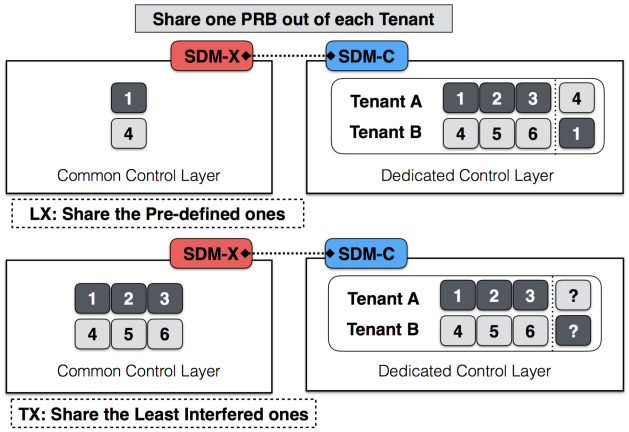


Fig. 2: Two sharing mechanisms explanation: in this example each tenant share only one of its PRB. In LX, two sharing PRBs (1 & 4) are specified manually but, in TX, the sharing PRBs are decided optimally and dynamically during operation

slice based resource management; on the other hand, SDM-X refers to the inter-slice controller operating in the common control layer, which is in charge of inter-slice resource management. Both controllers can work either separately or congruently, depending on the service request. As with respect to our work, the inter-tenant resource sharing framework should operate by proper coordination between SDM-X and SDM-C. With the programability and softwarization of SDN, optimization and well-designed algorithms like the proposed ones can be embedded into virtualization control layers to engage system improvement. As already mentioned above, these SDN controllers can be implemented as VNFs.

### B. Operation Mechanisms: Loose Coupling (LX) and Tight Coupling (TX)

Based on the virtual controllers described previously, we hereby introduce two different operation mechanisms under the framework of the proposed inter-tenant resource sharing and variable power allocation.

*1) Loose Coupling (LX):* LX operation refers to the scenario where inter-tenant sharable resources are pre-defined before the system operation. Therefore inter-slice control functionalities provided by SDM-X need to be set up before the operation of the optimization or algorithmic framework. Once the operation begins, LX assigns PRBs to users and allocates a proper transmission power within a defined power range to the assigned PRB based on an optimal reuse principle. By choosing a proper transmission power, more PRBs reuse can be engaged and interference can be further limited.

*2) Tight Coupling (TX):* This case is recognized when resources of individual tenants and shared ones are decided dynamically during the operation. Computationally TX is the most complex one in operation and requires a fully functional overlap between the SDM-C and SDM-X controllers. Compared to LX, TX only has the information about the amount of sharable resources before operation, and which PRBs shared in each tenant can be consistently changed according to resource re-usability, system interference and traffic conditions. The variable transmission power is also available in TX mode to engage the reuse of resources.

In terms of resource sharing, in LX, the SDM-C controller splits the bandwidth into different partitions to tenants, meanwhile, the SDM-X controller optimizes the reuse of the predefined inter-tenant sharable resources. On the other hand, in TX, the SDM-X controller takes all resources into account to find the optimal subset for sharing in each operation period. This distinction is depicted via a toy example shown in Fig.2. In essence, TX is considered as the most general and complex case for resource sharing, where a defined number of resources can be shared, but without depicting which ones from the full available set of resources. Therefore, in terms of network management, the trade off or implementation preference between TX and LX can be evaluated based on both sharing flexibility and operation complexity.

## III. System Model and Problem Formulation

This work considers a C/U split SDN architecture where SBSs are densely deployed in a centralized MBS controlling area. For this reason, and without loss of generality, we can ignore the inter-tier interference to simplify the model. In a C/U split network, the data plane (SBSs) focuses only on the forwarding user data rate while the control plane (MBSs) provide control functionalities. All SBSs in the network utilize a common frequency band (frequency reuse is allowed), which is different from the one used by MBS [7]. In terms of the topology we assume a number of $K$ SBSs distributed in the MBS area based on a Poisson Point Process (PPP) [34] recognized as user hot zones, and a number of $N$ user (UEs) that are randomly located in the hot zone SBSs. To serve the arrival traffic, the control plane creates a centralized resource pool based on the bandwidth of SBSs and SPs/tenants registered in this network can require virtual resources from the pool. In this case, the SPs serve their subscribers via the SBSs that provide the best signal link. The number of PRBs $M$ in the pool is directly dependent on system bandwidth and only downlink traffic is considered in this work.

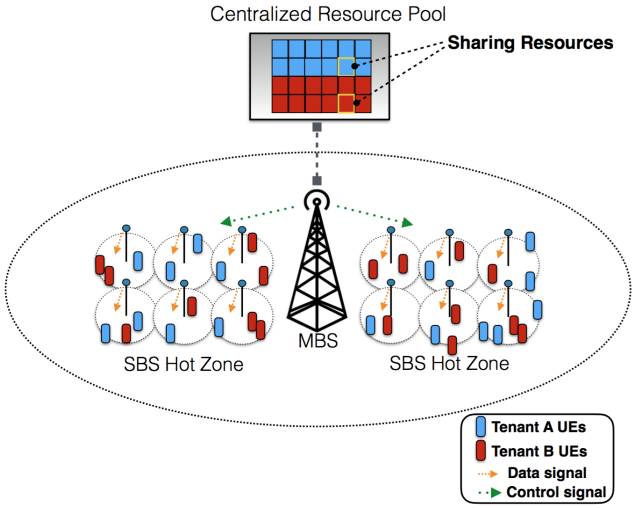


Fig. 3: An example of C/U split RAN architecture with traffic from two tenants: MBS controls SBSs which forward user data in hot zones and builds the centralized resource pool

An example of the network topology described above is shown in Fig.3. The available PRBs and UEs of two tenants (A and B) are colored blue and red, respectively. In the resource pool, two marked PRBs are those chosen to be shared between tenants in this example.

### A. Preliminaries

To model the resource association and power allocation problem in a mathematical programming setting, we define the following binary decision variables.

$$\mathbf{x_{rt}} = \begin{cases} 1 & \text{if PRB } r \text{ is assigned to tenant } t. \\ 0 & \text{otherwise.} \end{cases} \tag{1}$$

$$\mathbf{y_{irtl}} = \begin{cases} 1 & \text{if user } i \text{ of tenant } t \text{ uses PRB } r \text{ with power level } l. \\ 0 & \text{otherwise.} \end{cases} \tag{2}$$

Notations $\mathbf{I}$, $\mathbf{C}$, $\mathbf{T}$ and $\mathbf{P}$ are used to indicate the set of UEs, PRBs, tenants and power level, respectively. In this paper, only mathematical sets and decision variables are written in bold style. Besides, we assumed discretized power level denoted by the index $l$ [35] to embrace the nature of integer linear program. In this case, a power value $p^{i'}_{irtl}$ represents a controllable transmission power by the base station when serving user $i$, and $i$' indicates the cell connected to user $i$. Previous research in [36] shows the details of how a PRB can be allocated a variable power by using discrete power levels. As mentioned before, we have $|\mathbf{C}| = M$ PRBs in the resource pool, $|\mathbf{P}|$ power levels and $|\mathbf{B}| = K$ SBSs (in a set $\mathbf{B}$) waiting to serve a number of $|\mathbf{I}| = N$ users from a number of $|\mathbf{T}|$ tenants, then the potential maximum power of each PRB is $p^{max}_{irtl} = P_{tx}/M$. The notation $P_{tx}$ denotes the maximum transmission power of a SBS; in our case all SBSs have the same maximum transmission power. Based on this, the variable transmission power that can be allocated to each PRB is defined as follows,

$$p^{i'}_{irtl} \leq p^{max}_{irtl} \tag{3}$$

Furthermore, we define the following indicator to express the orthogonal resource reuse principle,

$$\phi_{ij}^{tt'} = \begin{cases} 1 & \text{if users i, j of tenants t and t' in different BSs.} \\ 0 & \text{otherwise.} \end{cases} \tag{4}$$

In this case, if users $i$ and $j$ belong to the same tenant then we have $t = t'$. Regarding the channel gains on downlink transmissions, we denote by $g_{irtl}^{i'}$ the link gain between the serving base station $i'$ and user $i$ using PRB $r$. Also, with $g_{irtl}^{j'}$ we denote the link gain between the serving base station of user $j$ (base station $j'$) and user $i$ as the interference link. There is no cross-tier interference due to the no data forwarding nature of MBS. In that respect, the signal to interference and noise ratio (SINR) for a PRB-UE pair can be estimated by the following expression,

$$\gamma_{irtl} = \frac{g_{irtl}^{i'} p_{irtl}^{i'} \mathbf{y_{irtl}}}{\sum_{j \in \mathbf{I'}} \sum_{t' \in \mathbf{T}} \sum_{l \in \mathbf{P}} \phi_{ij}^{tt'} g_{irtl}^{j'} p_{irtl}^{j'} \mathbf{y_{jrt'l}} + I_{noise}} \tag{5}$$

The terms $\gamma_{irtl}$ and $I_{noise}$ indicates the SINR and the background noise of the channel, respectively. We note that the set $\mathbf{I'}$ represents the user set without user equipment (UE) $i$.

Based on Eq.(5), the achievable data rate of UE $i$ by taking PRB $r$ can be approximated by the Shannon Capacity Formula,

$$R_{irtl}(\mathbf{y_{irtl}}) = \Delta f log_2(1 + \gamma_{irtl}) \tag{6}$$

where $\Delta f$ is the LTE-based frequency space for a PRB [37]. Comparing to previous research [38][39] using the aggregated energy as the energy measurement metric, we utilize the Energy Efficiency (EE) metric, since it indicates both the energy consumption and user data rate [40]-[43]. Based on the accumulated energy consumption and aggregated user data rate, the EE in this work is defined as follows,

$$EE = \frac{\sum_{i \in \mathbf{I}} \sum_{r \in \mathbf{C}} \sum_{t \in \mathbf{T}} \sum_{l \in \mathbf{P}} R_{irtl}(\mathbf{y_{irtl}})}{\sum_{i \in \mathbf{I}} \sum_{r \in \mathbf{C}} \sum_{t \in \mathbf{T}} \sum_{l \in \mathbf{P}} p_{irtl}^{i'} + \sum_{k \in \mathbf{B}} P_{SBS}^{k}} \tag{7}$$

The term $P_{SBS}^{k}$ represents the circuit/operation power of each SBS [42][43]. The unit of $EE$ is bit/Joule or Mbit/Joule.

### *B. Problem Formulation*

Based on the previously defined network modelling, the proposed resource reuse maximization problem can be defined as follows,

$$[\textbf{Problem I}] \ \max \sum_{i \in \mathbf{I}} \sum_{r \in \mathbf{C}} \sum_{t \in \mathbf{T}} \sum_{l \in \mathbf{P}} \mathbf{y_{irtl}} \tag{8}$$

s.t.

$$\sum_{r \in \mathbf{C}} \mathbf{x_{rt}} \geq n_t, \ \forall t \in \mathbf{T} \tag{8a}$$

$$\sum_{t \in \mathbf{T}} \mathbf{x_{rt}} \leq \beta, \ \forall r \in \mathbf{C} \tag{8b}$$

$$\sum_{r \in \mathbf{C}} \sum_{l \in \mathbf{P}} \mathbf{y_{irtl}} \leq \delta, \ \forall i \in \mathbf{I}, \forall t \in \mathbf{T} \tag{8c}$$

$$\sum_{r \in \mathbf{C}} \sum_{l \in \mathbf{P}} \mathbf{y_{irtl}} \geq 1, \ \forall i \in \mathbf{I}, \forall t \in \mathbf{T} \tag{8d}$$

$$\sum_{r \in \mathbf{C}} \sum_{t \in \mathbf{T}} \mathbf{x_{rt}} \leq \sum_{t} n_t + \alpha \tag{8e}$$

$$\mathbf{y_{irtl}} \leq \mathbf{x_{rt}}, \ \forall i \in \mathbf{I}, \forall r \in \mathbf{C}, \forall t \in \mathbf{T}, \forall l \in \mathbf{P} \tag{8f}$$

$$\gamma_{irtl}(\mathbf{y_{irtl}}) \geq \gamma_{th}, \ \forall i \in \mathbf{I}, \forall r \in \mathbf{C}, \forall t \in \mathbf{T}, \forall l \in \mathbf{P} \tag{8g}$$

$$\mathbf{y_{irtl}} + \mathbf{y_{jrtl}} \leq 1 + V \cdot \phi_{ij}^{tt'}, \forall i, j \in \mathbf{I}, \forall r \in \mathbf{C}, \forall t \in \mathbf{T}, \forall l \in \mathbf{P} \tag{8h}$$

$$\mathbf{x_{rt}} \in \{0, 1\} \tag{8i}$$

$$\mathbf{y_{irtl}} \in \{0, 1\} \tag{8j}$$

Constraint (8a) ensures that every tenant will be allocated at least $n_t$ orthogonal PRBs as agreed by a Service Level Agreement (SLA). Constraint (8b) indicates that a PRB can be reused up to $\beta$ times across all tenants, which is one way to manage network interference. Furthermore, constraint (8c) aims to limit the potential intra-tenant interference by ensuring that up to $\delta$ PRBs can be associated to one UE per tenant. Constraint (8d) indicates for each UE should at least take one PRB as a successful channel connection. Constraint (8e) ensures that only up to $\alpha$ PRBs can be shared between tenants; this can be set by the InP according to some predefined policies or rules. The binding constraint between the decision variables $y_{irtl}$ and $x_{rt}$ is expressed in (8f). Constraint (8g) expresses the SINR threshold $\gamma_{th}$ that need to be satisfied in order to use a PRB. Constraint (8h) defines that users from the same tenant and different tenants should be allocated a different PRB if they connect to the same SBS (same cell avoidance) and $V$ in this case is an arbitrary large integer. Constraints (8i) and (8j) ensure that the variables are binary. To guarantee constraint (8g) is always satisfied when $y_{irtl}$ = 0, $\gamma_{irtl}$ is re-written as follows,

$$\gamma_{irtl} = \frac{g_{irtl}^{i'} p_{irtl}^{i'} \mathbf{y_{irtl}} + V(1 - \mathbf{y_{irtl}})}{\sum_{j \in \mathbf{I'}} \sum_{t' \in \mathbf{T}} \sum_{l \in \mathbf{P}} \phi_{ij}^{tt'} g_{irtl}^{j'} p_{irtl}^{j'} \mathbf{y_{jrt'l}} + I_{noise}} \tag{9}$$

In this optimization problem, note that we maximize the amount of reusable resource blocks with SINR restriction rather than directly optimize the data throughput. Even so, we can still have promising gains in terms of throughput, since our proposal aims to ultimately reuse inter slice resources compared to the present state of the art in the scope area. However, we note that this gain might not be guaranteed all the time as in our previous work [30], which performs the same optimization but with constant transmission power. To this end, the following result is contributed to shed light on this issue.

*Lemma 1: Under the proposed inter-tenant resource sharing framework, the maximum system rate can be possibly provided by the non-reuse case with constant power rather than the reuse case with power control in certain scenarios.*

**Proof:** See Appendix. □

### C. Mathematical Differences between LX and TX

The above problem formulation is the one describing mathematically the TX mode of operation, since the inter-tenant sharing subset is completely decided by the optimization problem itself. There is no pre-defined subset of resources that decide which PRBs are sharable or belong to a certain tenant. With this understanding, we illustrate the difference between LX and TX in terms of formulation based on their available PRBs set:

• **TX Optimization**: Problem I is the exact mathematical expression for TX operation. To be noted, the set of PRBs that users and tenants can use coincide, which is $\mathbf{C}$.

• **LX Optimization**: The LX mode of operation has the same objective function and constraints as the TX operation, except the different PRB set for each tenant $t$, defined as $\mathbf{C_t}$. In the PRBs subset $\mathbf{C_t}$ of a tenant, the pre-defined sharable PRBs are marked manually before operation starts. Regarding to Problem I, the resource set $\mathbf{C}$ shall be replaced by $\mathbf{C_t}$ in all constraints when considering different $t$.

## IV. Resource and Power Joint Allocation (RPJA)

In this section, we propose two algorithms with different complexity to solve the optimization problem in polynomial time due to the NP-hardness of the optimization framework. Both algorithms aim to allocate PRBs and variable power to UEs jointly, therefore we name them the Resource and Power Joint Allocation algorithms (RPJA). In addition, to offer fair comparison between this work and our previous work [30] we further illustrate the resource allocation only version of these two algorithms (called RA algorithms) to realize constant power resource allocation in our previous optimization problem.

### A. RPJA-h and RA-h: Greedy based Heuristic

The proposed optimization problem is classified as a knapsack problem due to the nature of assigning discrete PRBs and power levels. Therefore, to explore the sub-optimal solutions in polynomial time, we firstly propose a simplified greedy based heuristic algorithm named RPJA-h. The procedure of conducting RPJA-h is shown in the pseudo code Algorithm 1: in step 1, RPJA-h randomly selects one PRB from set $\mathbf{C}$ and associates it with a UE requiring minimum power to pass its SINR threshold; in this way, the lowest interference will be generated at this stage. The association is made if all the constraints in the optimization problem are satisfied. In terms of power, a minimum power $p_{irtl}^{min}$ with a slack $S$ (a small portion of $p_{irtl}^{min}$) is allocated to the PRB-UE pair which ensures the connection would not be lost because of the future reuse of this PRB. Meanwhile, the potential interference will be quantified and saved to an interference matrix $H_{N\times N}$ in which each interfering user pair is indicated by $h_{ij}$ elementally. The matrix is in the form shown in Eq.(10) for a $N$ users system:

$$H_{N\times N} = \begin{bmatrix} 0 & h_{12} & \dots & h_{1N} \\ h_{21} & 0 & \dots & h_{2N} \\ \vdots & \vdots & \ddots & \vdots \\ h_{N1} & h_{N2} & \dots & 0 \end{bmatrix} \tag{10}$$

With the updated $H_{N\times N}$, the remaining unassociated UEs will be sorted again based on the present system interference until no more association can be made. This step ends when all PRBs are considered. In step 2, the sum rate of all associations $R_h$ is calculated. This algorithm can also be called an interference based greedy algorithm because the sorting is based on $H_{N\times N}$. To compare with our previous work [30], RPJA-h has another version without variable power allocation (PRB association only) named RA-h. The only difference RA-h has in Algorithm 1 is that RA-h allocates maximum transmit power $p_{irtl}^{max}$ to association pair instead of $(1+S)p_{irtl}^{min}$ through the whole process. As can be seen, RPJA-h engages more resource reuse compared to RA-h due to its stricter interference control.

**Algorithm 1:** RPJA-h

**Data:** Location coordinates of UEs and SBSs; network parameters $n_t$, $\beta$, $\delta$, $\alpha$ and $\gamma_{th}$; Interference matrix $H_{N\times N} = \emptyset$, PRBs set $\mathbf{C}$ and UEs set $\mathbf{I}$.
**Result:** PRBs Association, Power Allocation and Rate Estimation.

Step 1: PRB Association and Power Allocation
**for** *r:=1 to* $M \in \mathbf{C}$ **do**
  • sort elements (ascending) in $\mathbf{I}$ based on $p_{irtl}^{min}$;
  **for** *i:=1 to* $N \in \mathbf{I}$ **do**
    **repeat**
      • obtain location and channel information of UE $i$;
      • allocate power $(1+S)\ p_{irtl}^{min}$ from nearest SBS;
      **if** ($\phi_{ij}^{tt'} = 1$ & $\gamma_{irtl} \geq \gamma_{th}$ *for all associated users)* **then**
        • $y_{irtl}$ =1, PRB $r$ is assigned to UE $i$;
        • $x_{rt}$ =1, Mark PRB $r$ used by tenant $t$;
        • update matrix $H_{N\times N}$;
        • sort remaining elements (ascending) $i+1$ to $N$ in $\mathbf{I}$ based on $H_{N\times N}$;
      **else**
        • $y_{irtl}$ & $x_{rt}$ = 0, no association made
      **end**
    **until** $\delta, \beta$ ***or*** $(n_t + \alpha)$ *is reached*;
  **end**
  • $H_{N\times N} = \emptyset$, clear the interference matrix for next PRB;
**end**
Step 2: Compute Sum Rate
• $R_h = \sum R_{irtl} y_{irtl}$

**Algorithm 2:** RPJA-adv

**Data:** Location coordinates of UEs and SBSs; network parameters $n_t$, $\beta$, $\delta$, $\alpha$ and $\gamma_{th}$; Interference matrix $H_{N\times N} = \emptyset$, PRBs set $\mathbf{C}$ and UEs set $\mathbf{I}$.
**Result:** PRBs Association, Power Allocation and Rate Estimation.

Step 1: PRB association and Power Allocation
**for** *z:=1 to Z* **do**
- generate a random number $\zeta$ between 0 and 1;
- **for** *r:=1 to* $M \in \mathbf{C}$ **do**
  - conduct the transformation in Eq.(11) and Eq.(13) based on $p_{irtl}^{min}$ and generate $D_i$ for all UEs;
  - sort elements (ascending) in $\mathbf{I}$ based on the distance between $\zeta$ and $D_i$;
  - **for** *i:=1 to* $N \in \mathbf{I}$ **do**
    - **repeat**
      - obtain location and channel information of UE $i$;
      - allocate power $(1+S)\ p_{irtl}^{min}$ from nearest SBS;
      - **if** *(*$\phi_{ij}^{tt'} = 1$ *&* $\gamma_{irtl} \geq \gamma_{th}$ *for all associated users)* **then**
        - $y_{irtl}$ =1,PRB $r$ is assigned to UE $i$ ;
        - $x_{rt}$ =1,Mark PRB $r$ used by tenant $t$;
        - update matrix $H_{N\times N}$;
        - conduct the transformation in Eq.(11) and Eq.(13) based on interference in $H_{N\times N}$ and generate $D_i$ for remaining UEs;
        - sort unassociated elements (ascending) in $\mathbf{I}$ based on the distance between $\zeta$ and $D_i$;
      - **else**
        - $y_{irtl}$ & $x_{rt}$ = 0, no association made
      - **end**
    - **until** $\delta, \beta$ ***or*** $(n_t + \alpha)$ *is reached*;
  - **end**
  - $H_{N\times N} = \emptyset$, clear the interference matrix for next PRB;
- **end**
- $R_{(z)} = \sum R_{irtl} y_{irtl}$;

**end**

Step 2: Provide Best Performed Sum Rate
- $R_{adv} = \max\{R\}$

### *B. RPJA-adv and RA-adv: Advanced Iterative Heuristic*

To improve the performance of RPJA-h, we further design an advanced iterative algorithm named RPJA-adv. The procedure of implementing RPJA-adv is illustrated in Algorithm 2. The key difference between RPJA-adv and RPJA-h is that RPJA-adv randomly changes the sorting result in RPJA-h with certain probabilities in each iteration $z$, thus better PRB-UE association can be expected.

In order to augment the algorithm with the proposed probabilistic selection, a set of mathematical transformations is proposed accordingly. A parameter named critical decision value $d_i'$ for each UE $i$ is defined as follows,

$$d_i = 1 - \frac{E_i}{E_{max}} \tag{11}$$

$$d_i' = \frac{d_i}{\sum_{i\in\mathbf{I}} d_i} \tag{12}$$

$E_i$ indicates the sorting element of corresponding UE $i$ which can be either $p_{irtl}^{min}$ or aggregated interference in $H_{N\times N}$ for this UE, and $E_{max}$ indicates the maximum element among all candidate users. Once $d_i'$ for all users has been decided, a critical selection range for each UE is derived as $D_i$. The first sorted user has critical selection range $D_1 \in [0, d_1']$ and $D_i \in [d_{i-1}', d_i' + d_{i-1}']$ is the one for the rest of users. As shown in Algorithm 2, step 1 begins with uniformly generating a random number $\zeta$ between 0 and 1 for each iteration $z$, then the critical selection range $D_i$ is found for each UE by Eq.(11) based on $p_{irtl}^{min}$. In this case the sorting of users is carried out depended on the distance between $\zeta$ and each $D_i$. With this sorting result, PRB-UE association will be made and minimum power with a slack will be allocated as in RPJA-h. It is important to note that the same sorting decision with mathematical transformation is conducted based on interference matrix $H_{N\times N}$ for the remaining users until no more association can be made afterwards. At the end of step 1 the sum rate for each iteration $z$ is estimated and saved to database, and in step 2 the result of the best sum rate iteration will be generated as final output of RPJA-adv. Similarly, another version of RPJA-adv with constant power allocation is also designed, as RA-adv.

Similar to Problem Formulation, both algorithms shown in this section are based on the TX mode of operation. For the LX operation, the subset of available PRBs shall be decided based on the requirements from users, which are assumed to be known by the network controller (obtaining location and state channel information of the users).

## V. Numerical investigations

The numerical investigations have been conducted based on a wide set of varied scenarios with a realistic set of parameters from 3GPP. We firstly explain the system environment and assumptions that realize a C/U split wireless network. Secondly, a set of large scale realistic network simulations is presented, in which we compare the RPJA and RA embedded LX and TX with classic network slicing methods in terms of the different performance perspectives. Lastly, we further illustrate improvement limits, optimality, complexity and scalability of proposed optimization problem and algorithms by introducing a small scale network simulation.

### *A. Simulation Scenarios and System Model Parameters*

The simulated wireless network environment follows the LTE-Advanced network principles proposed by 3GPP [12]. In all simulated scenarios the widely used 10 MHz channel bandwidth is adopted, which provides in total 50 available

PRBs. To realize the C/U split RAN network, a cluster of SBSs is deployed in a MBS (located at the center) controlling area. The number of SBSs varies from 3 to 15 and the deployment follows a Poisson Point Process (PPP). The selected SBSs are standard pico cells that serve traffic in hot zones. We assume the base station transmits with its maximum power in the case without power control and only the downlink is considered. A summary of used parameters can be found in Table I. The custom Monte Carlo based simulation has been designed and implemented in MATLAB. In each iteration, UEs from two tenants are randomly distributed in the hot zones. The SINR threshold is decided by the average channel conditions of all users in each iteration. In addition, according to [44], the general used maximum transmission power of a pico cell is 0.25 W and the circuit power of each is 14.9 W. In order to provide

TABLE I: SIMULATION SPECIFICATION AND PARAMETERS

| **Parameters** | Values / Assumptions |
|---|---|
| Network layout | 1 MBS with 3 - 15 SBSs |
| Cell radius (m) | MBS:1000 SBS: 200 |
| Carrier frequency (GHz) | 2 |
| MBS antenna gain (dBi) | 14 |
| SBS antenna gain (dBi) | 10 |
| Antenna configuration | 1 Tx for BS, 1 Rx for UE |
| Thermal noise (dBm/Hz) | -174 |
| System Bandwidth (MHz) | 10 |
| No. of PRBs in the pool | 50 |
| SBS Path loss (dB) | $140.7+36.7\log_{10}(D)$ (D in km) |
| MBS Path loss (dB) | $128.1+36.7\log_{10}(D)$ (D in km) |
| Shadowing standard deviation (dB) | 6 |
| Max SBS TX power (dBm) | 24 |
| MBS TX power (dBm) | 43 |
| Number of UEs | 50 - 150 |
| Max No. of a PRB reuse | 5 |
| Max No. of UE requirement for PRBs | 2 |

a holistic view on attainable performance, we compare our proposed algorithms with two nominal virtual resource slicing approaches in virtual network for a two tenants scenario. These are the resource based NVS (NVS-RB) scheme and the static reservation (SR). As mentioned in the introductory section, the NVS-RB [20] offers certain flexibility in network slicing; it initially reserves a proportion of resources for each slice but automatically transfers resources between slices based on traffic conditions (dynamic resource requirement of each tenant). On the other hand, in the SR based slicing approach the resources for each slice are fixed and remain constant independently of traffic variations. The advantage of NVS-RB is the self-reacting adjustment for slicing resources based on incoming traffic; therefore, in all simulation scenarios our LX and TX mechanisms will be embedded on the top of NVS-RB by slicing PRBs in resource pool before enabling inter-tenant sharing. In summary, for all scenarios, the performance evaluations are compared among the following cases: LX and TX (using RPJA-h, RPJA-adv, RA-h and RA-adv), NVS-RB and SR. The results are presented by the mean value of data observations. To ensure the analysis credibility, we also calculate the confidence interval (CI) and statistical error (SE) in each numerical result section by using 95% confidence level (CL) [45][46]. The formula of CI is shown in Eq.(13) below:

$$CI = \bar{x} \pm z\frac{\sigma}{\sqrt{n}} \tag{13}$$

where $\bar{x}$ is the mean value of observations, $z$ is the z statistic, $\sigma$ is the standard deviation and $n$ is the number of observations.

## B. Performance Evaluation

### 1) System Throughput Performance:

In this large scale simulation, we show the network performance of 6 SBSs scenarios. Besides, the number of UEs is varied from 50 to 150 as traffic load. To be noted, we applied 10 PRBs (20% of total resources) as the total amount of inter-tenant sharing PRBs, the parameter $\alpha$, among two tenants registered in the network.

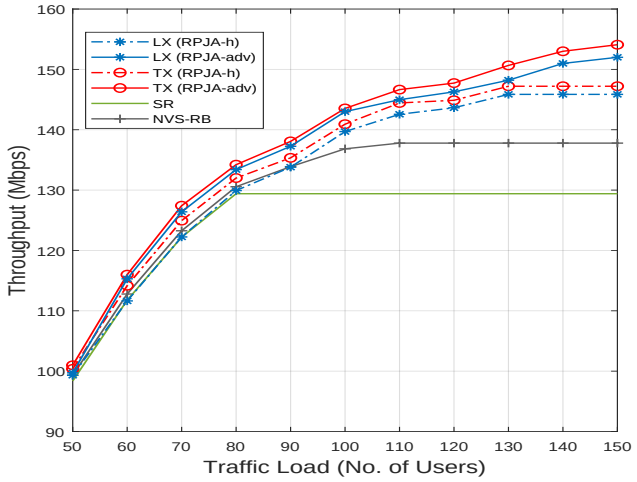


(a) RPJA throughput

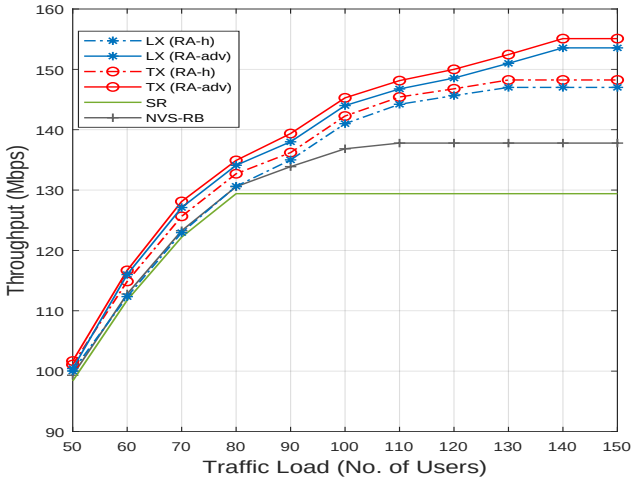


(b) RA throughput

Fig. 4: Throughput performance of both RPJA and RA algorithms

Fig.4a and Fig.4b show the cumulative throughput of variable power allocation (RPJA) and constant power allocation (RA). As may be observed, the total throughput in all cases increases with the traffic load due to the increasing

number of UEs in the network. Note, however, that the throughput reaches a saturated status at certain traffic load since the UEs' requirement exceeds the available PRBs in resource pool for all cases. As expected, our proposed LX and TX embedded in both RPJA-adv and RA-adv methods are the last saturated methods in very congested traffic with around 140 UEs. Meanwhile, with slight loss of maximum throughput of LX and TX both RPJA-h and RA-h methods are saturated at around 130 UEs, still outperforming the SR (saturated at 80) and NVS-RB (saturated at 100) schemes. As shown in Fig.4a, TX (RPJA-adv), LX (RPJA-adv), TX (RPJA-h) and LX (RPJA-h) achieve the maximum system throughput of 154.1 Mbps, 152 Mbps, 147.2 Mbps and 144.9 Mbps, respectively, at their saturated point, which translates to maximum throughput gains 19.5%, 17.8%, 14.1% and 12.3% compared to SR (129 Mbps), and 11.6%, 10.07%, 7.4% and 4.9% compared to NVS-RB (138.1 Mbps). Note that with slightly higher gains (see Fig.4b), the maximum throughput of TX (RA-adv), LX (RA-adv), TX (RA-h) and LX (RA-h) outperformed SR by 20.6%, 18.6%, 15.3% and 14.0%, and NVS-RB by 12.10%, 12.7%, 8.0% and 6.2%. As stated in Lemma 1, the RA embedded methods with constant power can have slightly higher sum rates compared to the RPJA embedded methods with power control due to the dynamic network traffic. In addition, LX usually loses 1-3% throughput compared to TX embedded in all methods due to the flexibility in choosing the shareable PRBs of TX. The margin error of this result is ranged from around -2.4 Mb/s to 2.2 Mb/s, contributing maximum 2.4% variation in data statistic.

*2) Per User Rate Performance:*

In Fig.5(a-d), we present the per user achievable rate based on the cumulative distribution function (CDF). For simplicity of presentation, in this part we only compare TX embedded in all algorithms and the nominal methods because the result of LX has the same trend and characteristics as TX. Among these figures, we focus on the CDF percentage of 1.5 Mbps point which can be seemed as a threshold dividing lower rate and higher rate. In terms of this specific point, Fig.5a and 5b show that both RPJA and RA based TX operation provide more users with higher data rate ($\geq$ 1.5 Mbps) compared to classic methods in a low traffic network scenario with 50 users, in which RA-adv, RA-h, RPJA-adv and RPJA-h have 68%, 62%, 65% and 60%, respectively, of total user population achieving data rate beyond the threshold compared to 44% and 52% of SR and NVS-RB, respectively. This result indicates that our proposed algorithms can not only improve the system throughput but also the individual user rate by engaging aggressive PRB reuse between tenants. Similarly, Fig.5c and Fig.5d indicate that even in a very congested traffic scenario with 150 users, TX embedded in RA-adv, RA-h, RPJA-adv and RPJA-h also generate 12%, 8%, 8.5% and 7.5% higher data rate UEs compared to SR and NVS-RB both with merely 5% higher data rate UEs. However, in this extreme congested scenario, not all UEs can be served with a satisfying rate or even connected to the SBSs due to the high interference environment and the lack of resources.

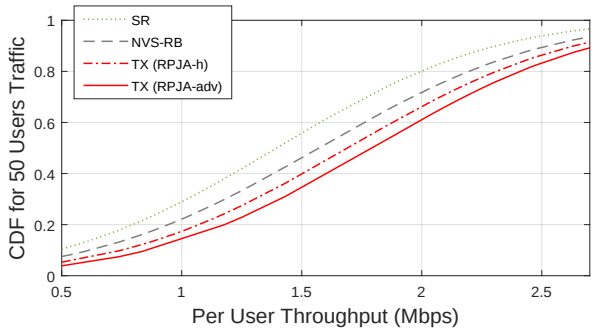


(a) RPJA based TX for 50 Users

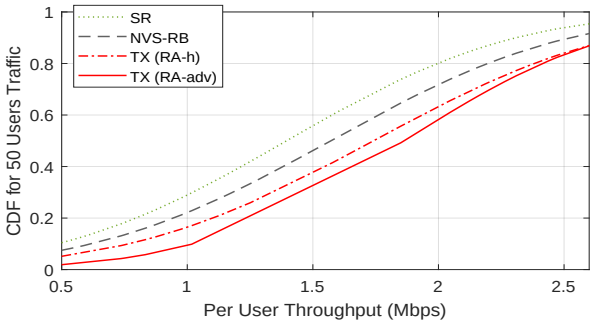


(b) RA based TX for 50 Users

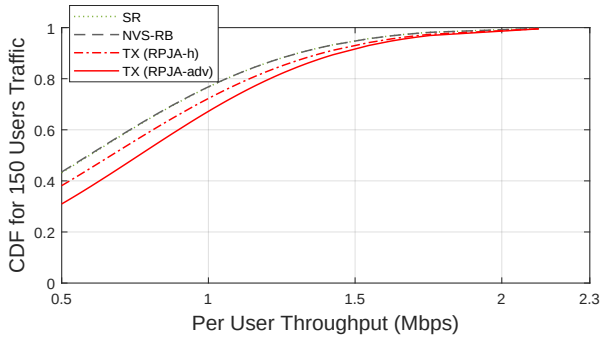


(c) RPJA based TX for 150 Users

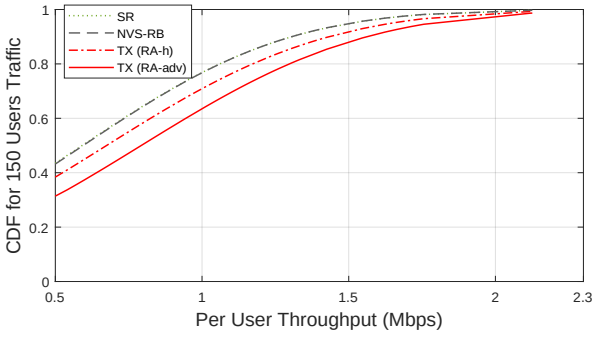


(d) RA based TX for 150 Users

Fig. 5: Per user rate performance of TX operation

*3) Energy Efficiency Performance:*

In this part, we evaluate the energy efficiency between

different methods to demonstrate the potential benefits of variable power algorithms. The EE result is shown as a set of box plots, using all traffic scenarios EE statistical data. In Fig.6, the EE of all methods with TX operation is illustrated. The reason for using only TX is still that there is no obvious difference in EE results between LX and TX operations in our simulation. We use the box plots to illustrate the variations of EE for all methods through the low traffic load scenario to the high traffic load scenario. Each box itself represents the EE value variation range, and the red band in the box indicates the median value. Some extreme values (i.e., outliers) are indicated by the red crosses.

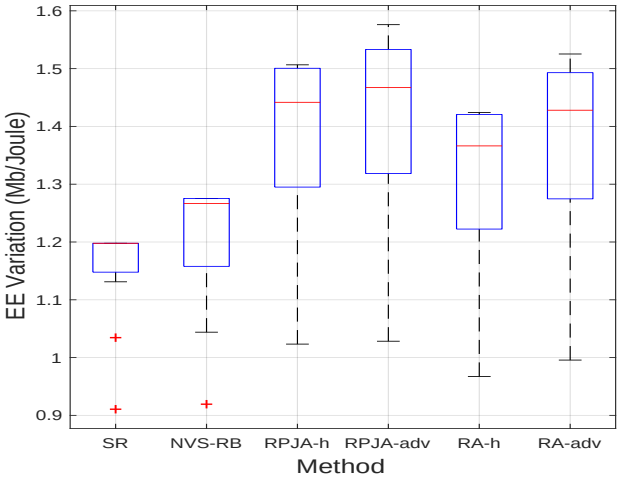


Fig. 6: Energy efficiency(EE) advantage of RPJA based TX

Without doubt, RPJA-adv has the best EE distribution (as shown in the box plot) and RPJA-h, RA-adv, RA-h ranks accordingly behind it. Such results indicate that the RPJA algorithms not only focus on motivating the reuse of PRBs but also lowering transmit power which can still satisfy the required received signal level . More specifically, RPJA-adv and RPJA-h provides the EE distribution from 1.32 to 1.53 and 1.29 to 1.50, respectively, compared to the one of RA-adv and RA-h from 1.27 to 1.49 and 1.23 to 1.42, respectively. As may be observed, RA-adv is the one with the closest distribution of RPJA algorithms, which is brought by its advantage in providing high rate. In terms of classic methods, we compared with, SR has the worst EE performance with distribution between 1.15 and 1.20; on the other hand, NVS has relatively higher distribution between 1.65 and 1.27 due to the relatively higher PRBs reuse efficiency. The error margin of EE value is ranged from -0.02 to 0.03, contributing a maximum 1.70% variation in data statistic.

*4) Parameter' Margin Study:*

In this set of numerical investigations, we study two parameters that potentially influence the performance of our proposed algorithms. Firstly, Fig.7a and Fig.7b show that the change of inter-tenant sharing capacity $\alpha$, ranged from no sharing to 14 PRBs sharing, can translate to a variation in system

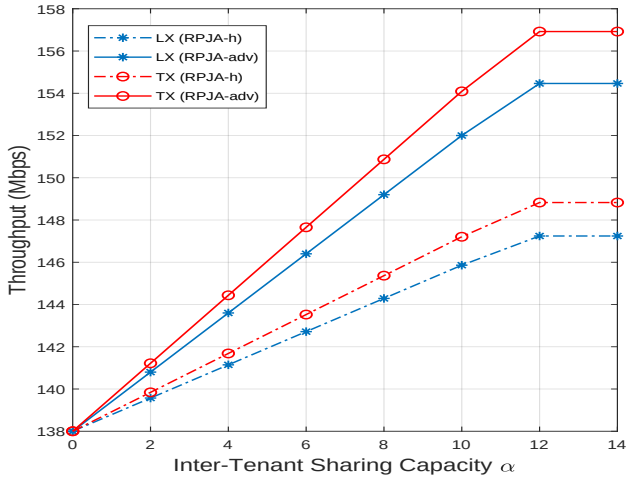


(a) RPJA Sharing Capacity

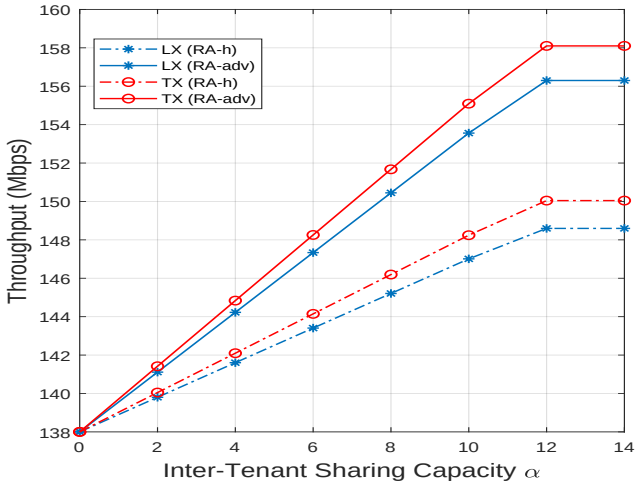


(b) RA Sharing Capacity

Fig. 7: Throughput improvement brought by changing sharing capacity of RPJA and RA for 150 users traffic load

throughput. In a highly congested network scenario with 150 users, Fig.7a indicates that the system throughput of RPJA algorithm, TX and LX based RPJA-adv and RPJA-h both increase the network throughput with respect to increasing sharable number of PRBs. However, they all comes to a saturated status with sharing capacity increased to 12. This happens because the total interference in the network reaches its cap; therefore, no more reuse could happen even though more sharable resources become available. Compared to no inter-tenant sharing scenario ($\alpha = 0$), which has system throughput of 138.1 Mbps, TX(RPJA-adv), LX (RPJA-adv), TX (RPJA-h) and LX (RPJA-h) improve system throughput by 13.7%, 11.7%, 7.8% and 6.6%, respectively, at their saturated point. Note that the same changing pattern also appears in the RA algorithm. Compared to the no sharing scenario, the maximum gains in throughput provided by TX (RA-adv), LX (RA-adv), TX (RA-h) and LX (RA-h) are 14.5%, 13.1%, 8.7% and 7.4%, respectively. The error margin of sharing capacity

results is very close to the throughput result, ranged from -2.3 Mb/s to 2.2 Mb/s.

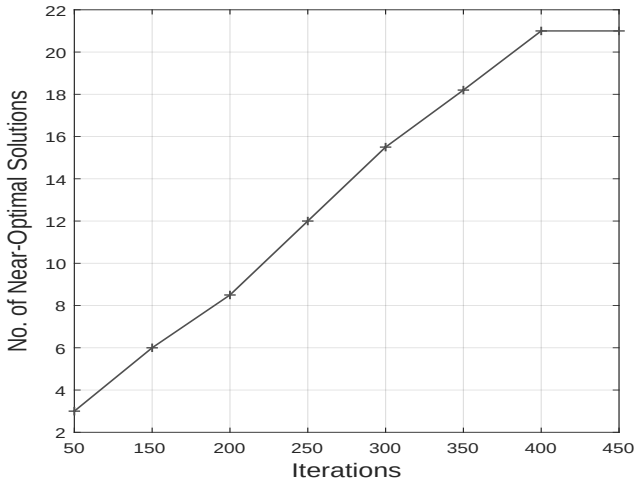


Fig. 8: Iterations applied by RPJA-adv and RA-adv algorithms for Searching the Solutions

Additionally, we study the efficiency of proposed RPJA-adv and RA-adv algorithms to locate a near-optimal solutions compared to RPJA-h and RA-h. In Fig.8, the curve was plotted based on the average number of both RPJA-adv and RA-adv near-optimal solutions compared to greedy heuristic results for different designated iterations $Z$. It can be easily understood that better solutions are obtained increasingly with the increasing iteration times from initially 50 iterations until 400 iterations are reached. The maximum number of near-optimal solutions found is around 21 on average and it is unchanged after 400 iterations mainly because of the searching limitation of both the RPJA-adv and RA-adv schemes.

### C. Small Scale Simulation: Optimality and Complexity

Finally, we present performance comparison between optimal solutions and the proposed algorithms in a small scale simulation where optimal solutions could be attained. The simulation was conducted based on an environment including 3 SBSs, 10 to 50 UEs traffic load, 10 available PRBs, totally 4 inter-tenant sharing PRBs and other unchanged parameters.

Fig.9a and Fig.9b show the system throughput of variable power allocation framework and constant power allocation framework, respectively. In both graphs, as expected optimal solutions (RPJA-OP and RA-OP) for both LX and TX show the similar developing trend of the algorithms but with higher throughput in value, which stems from the optimality provided by the solution of the proposed linear integer program. The maximum throughput improvement is still evaluated at the saturated point of all methods. In Fig.9a, the optimal solution LX(RPJA-OP) outperforms LX(RPJA-adv) and LX(RPJA-h) by 15.1% and 24.0%, respectively; On the other hand, optimal solution TX(RPJA-OP) outperforms TX(RPJA-adv) and TX (RPJA-h) by 14.5% and 24.2%, respectively. For constant power methods, Fig.9b shows that LX(RA-OP) outperforms

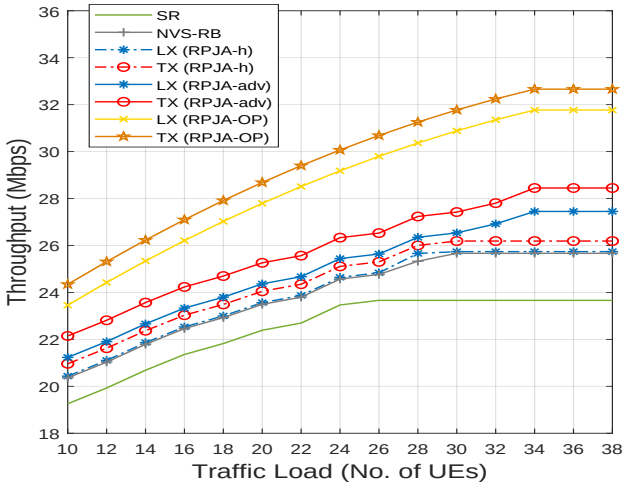


(a) RPJA based optimization and RPJA algorithm

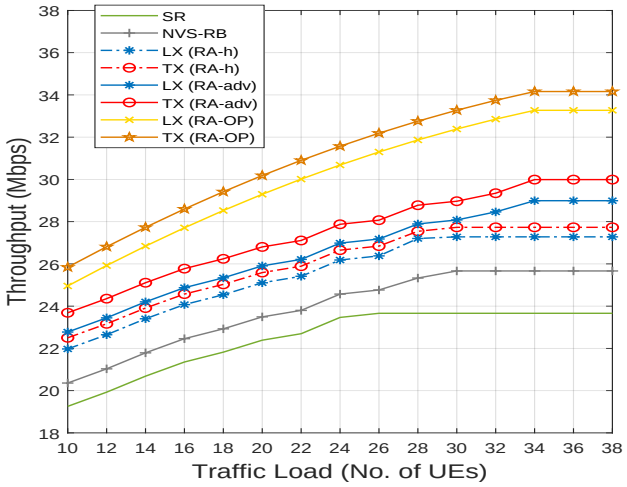


(b) RA based optimization and RA algorithm

Fig. 9: Throughput performance of the MILP based optimal solution and proposed heuristic algorithms in small scale simulation scenario.

LX(RA-adv) and LX(RA-h) by 14.5% and 19.0%, respectively, as well as TX(RA-OP) outperforms LX(RA-adv) and LX(RA-h) by 11.4% and 21.8%, respectively. The throughput performance compared with the SR and NVS-RB schemes is also summarized in Table II.

TABLE II: AVERAGE ENHANCEMENT IN SMALL SCALE SIMULATION

| **Methods** | Complexity | Gains on SR | Gains on NVS-RB |
|---|---|---|---|
| LX: RPJA-OP | NP-Hard | 27.2% | 19.5% |
| LX: RA-OP | NP-Hard | 33.9% | 25.9% |
| LX: RPJA-adv | $\mathcal{O}(\lvert\mathbf{I}\rvert\lvert\mathbf{C}\rvert Z)$ | 11.2% | 4.6% |
| LX: RA-adv | $\mathcal{O}(\lvert\mathbf{I}\rvert\lvert\mathbf{C}\rvert Z)$ | 18.1% | 11.0% |
| LX: RPJA-h | $\mathcal{O}(\lvert\mathbf{I}\rvert\lvert\mathbf{C}\rvert)$ | 6.8% | 1.3% |
| LX: RA-h | $\mathcal{O}(\lvert\mathbf{I}\rvert\lvert\mathbf{C}\rvert)$ | 13.7% | 6.9% |
| TX: RPJA-OP | NP-Hard | 30.2% | 23.3% |
| TX: RA-OP | NP-Hard | 34.9% | 29.6% |
| TX: RPJA-adv | $\mathcal{O}(\lvert\mathbf{I}\rvert\lvert\mathbf{C}\rvert Z)$ | 15.3% | 8.4% |
| TX: RA-adv | $\mathcal{O}(\lvert\mathbf{I}\rvert\lvert\mathbf{C}\rvert Z)$ | 22.2% | 14.9% |
| TX: RPJA-h | $\mathcal{O}(\lvert\mathbf{I}\rvert\lvert\mathbf{C}\rvert)$ | 8.9% | 2.4% |
| TX: RA-h | $\mathcal{O}(\lvert\mathbf{I}\rvert\lvert\mathbf{C}\rvert)$ | 15.8% | 8.9% |

Furthermore, the dimension of the optimization problem is $|\mathbf{C}|+|\mathbf{T}|+|\mathbf{C}||\mathbf{T}|+\mathbf{2}|\mathbf{I}||\mathbf{T}|+2|\mathbf{I}||\mathbf{C}||\mathbf{T}||\mathbf{P}|+|\mathbf{I}|^{\mathbf{2}}|\mathbf{C}||\mathbf{T}||\mathbf{P}|$, which makes optimal solution impossible to achieve in a real network. Table III shows an example of the scalability. However, the complexity of the proposed algorithms is simply decided by the number of iterations, users and resources (also see II). Therefore, by sacrificing a slight loss in a large scale network scenario, the performance of both greedy and iterative algorithms is acceptable. More information about the optimality and complexity can be found in Table II.

TABLE III: VARIABLES AND CONSTRAINTS SIZE SCALABILITY

| **Problem I dimension** | Variables | Constraints |
|---|---|---|
| M=5, N=5, $\|\mathbf{T}\|$=2, $\|\mathbf{P}\|$=3 | 160 | 1087 |
| M=10, N=10, $\|\mathbf{T}\|$=2, $\|\mathbf{P}\|$=3 | 620 | 7272 |
| M=10, N=50, $\|\mathbf{T}\|$=2, $\|\mathbf{P}\|$=3 | 3100 | 36192 |
| M=50, N=50, $\|\mathbf{T}\|$=2, $\|\mathbf{P}\|$=3 | 15100 | 780352 |

## VI. Conclusions

In this paper, a novel inter-tenant resource sharing method bound with a variable power allocation optimization framework is proposed. The significance of the framework lies on the fact that it allows to expand network capacity and user service available rate by reusing the physical resources between tenants incorporated with suitable power control policies. To allow different depth of resource sharing, two schemes have been proposed under a mathematical programming optimization framework. To eliminate the curse of dimensionality, scale-free resource and power joint allocation algorithms are designed amenable for real-time implementation and rigorous analysis via numerical investigations reveals significant performance gains compared to nominal network slicing schemes.

## Acknowledgement

This work has been partially funded by the H2020-ICT-2014-2 project 5G NORMA. The authors would like to acknowledge the contributions of their colleagues, although the views expressed are those of the authors and do not necessarily represent the project.

## Appendix

### A. Proof of lemma 1

In this case, a simplified mathematical model is shown to prove the statement in lemma 1. Eq.(14) shows the typical SINR calculation for a user $i$, where $\omega_1$ and $\omega_2$ are the power controlling ratio of the signaling cell and interfering cell respectively, ranged from 0 to 1. The parameters $g_i$ and $g_{i'}$ are antenna gains from the signaling cell and interfering cell for the user. Still, the two cells have the same maximum transmission power $p^{max}$.

$$\gamma_i = \frac{g_i \omega_1 p^{max}}{g_{i'} \omega_2 p^{max} + I_{noise}} \tag{14}$$

Assume an extreme scenario where two users are located in two adjacent cells with UE1 located at the edge of cell 1 ended up with an extremely small antenna gain $g_1$=1 and UE2 located at the center of cell 2 with an extremely high antenna gain as $g_2$=N, a large positive number. Moreover, assume that the antenna gain from the interfering cell for UE1 is $g_1 = 1$ (maximum interference) and for UE2 is $g_2 = \frac{1}{N}$. To further simplify the SINR calculation, assume that maximum transmission power $p^{max}$ for both cells is 1 and thermal noise $I_{noise}$ is $\frac{1}{N}$, which is small enough to be ignored. Following Eq.(14), the SINR for each user in this scenario can be expressed as,

$$\gamma_1 = \frac{g_1 \omega_1 p^{max}}{g_1' \omega_2 p^{max} + I_{noise}} \tag{15}$$

$$\gamma_2 = \frac{g_2 \omega_2 p^{max}}{g_2' \omega_1 p^{max} + I_{noise}} \tag{16}$$

With all the denoted values, Eq.(15) and Eq.(16) can be expresses as,

$$\begin{aligned} \gamma_1 &= \frac{\omega_1}{\omega_2 + \frac{1}{N}} \\ &= \frac{\omega_1 N}{\omega_2 N + 1} \end{aligned} \tag{17}$$

$$\begin{aligned} \gamma_2 &= \frac{\omega_2 N}{\frac{\omega_1}{N} + \frac{1}{N}} \\ &= \frac{\omega_2 N^2}{\omega_1 + 1} \end{aligned} \tag{18}$$

Based on the achieved SINR, the system sum rate can be calculated (aggregated rate of two users) as,

$$\begin{aligned} R &= \Delta f[log_2(1+\gamma_1) + log_2(1+\gamma_2)] \\ &= \Delta f[log_2(1+\frac{\omega_1 N}{\omega_2 N + 1}) + log_2(1+\frac{\omega_2 N^2}{\omega_1 + 1})] \end{aligned} \tag{19}$$

To compare with the non-reuse case, Eq.(19) can be rewritten to express the following scenarios: (1) only UE1 is served ($\omega_1$=1 and $\omega_2$=0) and (2) only UE2 is served (($\omega_1$=0 and $\omega_2$=1)).

The achievable rate for the $\omega_1$=1 and $\omega_2$=0 scenario is calculated as,

$$R_{(\omega_1=1 \& \omega_2=0)} = \Delta f log_2(1+N) \tag{20}$$

The achievable rate for the $\omega_1$=0 and $\omega_2$=1 scenario is calculated as,

$$R_{(\omega_1=0 \& \omega_2=1)} = \Delta f log_2(1+N^2) \tag{21}$$

If we start from the first scenario ($\omega_1$=1 & $\omega_2$=0), we can always obtain higher rate than the rate calculated in Eq.(20) by increasing $\omega_2$ from 0 to 1 in Eq.(19). On the other hand, if we start from the second scenario ($\omega_1$=1 & $\omega_2$=0), we can always obtain lower rate than the rate calculated in Eq.(21) by increasing $\omega_1$ from 0 to 1. In this case, it is true to say that either higher or lower rate can be achieved by reusing the PRBs between users with power control compared to non-reuse with a constant power/ maximum power under the proposed optimization framework. The achievable aggregated rate can be deeply influenced by the value of $N$.

□

## REFERENCES


[1] 5G radio access: Research and Vision, White paper, Ericsson, Stockholm, Sweden, 2013.

[2] J. G. Andrews et al., "What will 5G be?" IEEE J. Sel. Areas Commun., vol. 32, no. 6, pp. 1065-1081, Jun. 2014.

[3] C. Liang and F. R. Yu, "Wireless Network Virtualization: A Survey, Some Research Issues and Challenges," IEEE Communications Surveys & Tutorials, vol. 17, no. 1, pp. 358-380, 2015.

[4] "Network Sharing; Architecture and Functional Description, 3GPP TS 23.251, Rev. 13.0.0", Dec. 2014.

[5] G. Tseliou, F. Adelantado and C. Verikoukis, "Scalable RAN Virtualization in Multitenant LTE-A Heterogeneous Networks," in IEEE Transactions on Vehicular Technology, vol. 65, no. 8, pp. 6651-6664, Aug. 2016.

[6] X. Costa-Perez, J. Swetina, T. Guo, R. Mahindra and S. Rangarajan, "Radio access network virtualization for future mobile carrier networks," in IEEE Communications Magazine, vol. 51, no. 7, pp. 27-35, July 2013.

[7] Ishii, H. Kishiyama, Y. Takahashi, "A novel architecture for LTEB :C-plane/U-plane split and Phantom Cell concept," IEEE Globecom Workshop, 2012 IEEE, pp.624,630, 3-7 Dec. 2012

[8] Manli Qian, Yuanyuan Wang, Yiqing Zhou, Lin Tian, Jinglin Shi, "A super base station based centralized network architecture for 5G mobile communication systems", Digital Communications and Networks, Volume 1, Issue 2, 2015, Pages 152-159.

[9] M. Kalil, A. Al-Dweik, M. F. Abu Sharkh, A. Shami and A. Refaey, "A Framework for Joint Wireless Network Virtualization and Cloud Radio Access Networks for Next Generation Wireless Networks," in IEEE Access, vol. 5, pp. 20814-20827, 2017.

[10] J. S. Panchal, R. D. Yates and M. M. Buddhikot, "Mobile Network Resource Sharing Options: Performance Comparisons," in IEEE Transactions on Wireless Communications, vol. 12, no. 9, pp. 4470-4482, September 2013.

[11] E. J. Kitindi, S. Fu, Y. Jia, A. Kabir and Y. Wang, "Wireless Network Virtualization With SDN and C-RAN for 5G Networks: Requirements, Opportunities, and Challenges," in IEEE Access, vol. 5, pp. 19099-19115, 2017.

[12] M. Richart, J. Baliosian, J. Serrat and J. L. Gorricho, "Resource Slicing in Virtual Wireless Networks: A Survey," in IEEE Transactions on Network and Service Management, vol. 13, no. 3, pp. 462-476, Sept. 2016.

[13] Open Networking Foundation, "OpenFlow white paper: Software-Defined Networking: The new norm for networks," Palo Alto, CA, USA, 2012.

[14] W. Xia, Y. Wen, C. H. Foh, D. Niyato and H. Xie, "A Survey on Software-Defined Networking," in IEEE Communications Surveys & Tutorials, vol. 17, no. 1, pp. 27-51, Firstquarter 2015.

[15] L. Li, Z. Mao, and J. Rexford, "Toward software-defined cellular networks," Software Defined Networking (EWSDN), 2012 European Workshop on, pp. 712, Oct 2012.

[16] R. Mijumbi, J. Serrat, J. L. Gorricho, N. Bouten, F. De Turck and R. Boutaba, "Network Function Virtualization: State-of-the-Art and Research Challenges," in IEEE Communications Surveys & Tutorials, vol. 18, no. 1, pp. 236-262, Firstquarter 2016.

[17] C. Chen, "C-ran: The road towards green radio access network", White Paper, China Mobile, 2011

[18] M. Hadzialic, B. Dosenovic, M. Dzaferagic, J. Musovic, "Cloud-RAN: Innovative radio access network architecture", Proc. 55th Int. Symp. (ELMAR), pp. 115-120, 2013.

[19] H. Hawilo, A. Shami, M. Mirahmadi, R. Asal, "NFV: State of the art challenges and implementation in next generation mobile networks (vepc)", IEEE Netw., vol. 28, no. 6, pp. 18-26, Nov. 2014.

[20] R. Kokku, R. Mahindra, H. Zhang, S. Rangajaran, "NVS: A substrate for virtualizing wireless resources in cellular networks", IEEE/ACM Trans. Netw., vol. 20, no. 5, pp. 1333-1346, Oct. 2012

[21] RAN Sharing: NECs Approach towards Active Radio Access Network Sharing , 2013.

[22] X. Costa-Perez, J. Swetina, T. Guo, R. Mahindra, S. Rangajaran, "Radio access network virtualization for future mobile carrier networks", IEEE Commun. Mag., vol. 51, no. 7, pp. 27-35, Jul. 2013.

[23] T. Guo, R. Arnott, "Active LTE RAN sharing with partial resource reservation", Proc. IEEE 78th VTC Fall, pp. 1-5, Sep. 2013.

[24] H. Zhang, N. Liu, X. Chu, K. Long, A. H. Aghvami and V. C. M. Leung, "Network Slicing Based 5G and Future Mobile Networks: Mobility, Resource Management, and Challenges," in IEEE Communications Magazine, vol. 55, no. 8, pp. 138-145, 2017.

[25] V. Yazici, U. C. Kozat, and M. O. Sunay, "A New Control Plane for 5G Network Architecture with a Case Study on Unified Handover, Mobility, and Routing Management," IEEE Commun. Mag., vol. 52, no. 11, Nov. 2014, pp.76-85.

[26] X. Yang, Y. Liu, K. S. Chou and L. Cuthbert, "A game-theoretic approach to network slicing," 2017 27th International Telecommunication Networks and Applications Conference (ITNAC), Melbourne, VIC, 2017, pp. 1-4.

[27] S. M. A. Kazmi, N. H. Tran, T. M. Ho and C. S. Hong, "Hierarchical Matching Game for Service Selection and Resource Purchasing in Wireless Network Virtualization," in IEEE Communications Letters, vol. 22, no. 1, pp. 121-124, Jan. 2018.

[28] R. Kunst, L. Avila, E. Pignaton, S. Bampi and J. Rochol, "A Resources Sharing Architecture for Heterogeneous Wireless Cellular Networks," 2016 IEEE 41st Conference on Local Computer Networks (LCN), Dubai, 2016, pp. 228-231.

[29] I. Malanchini, S. Valentin and O. Aydin, "Generalized resource sharing for multiple operators in cellular wireless networks," International Wireless Communications and Mobile Computing Conference (IWCMC), Nicosia, 2014, pp. 803-808.

[30] Jinwei Gang and Vasilis Friderikos, "Optimal Resource Sharing in Multi-Tenant 5G Networks," IEEE Wireless Communications and Networking Conference (WCNC), Barcelona, 2018.

[31] Colazzo, A., Ferrari, R., and Lambiase, "Achieving low-latency communication in future wireless networks: the 5G NORMA approach", 2016

[32] ETSI NFV ISG, 'GS NFV-EVE 005 V1.1.1 Network Function Virtualisation (NFV); Ecosystem; Report on SDN Usage in NFV Architectural Framework', Dec. 2015

[33] 5GPPP Architecture Working Group, View on 5G Architecture, White paper, Dec, 2017.

[34] R. W. Heath, M. Kountouris and T. Bai, "Modeling Heterogeneous Network Interference Using Poisson Point Processes," in IEEE Transactions on Signal Processing, vol. 61, no. 16, pp. 4114-4126, Aug.15, 2013

[35] T. K. Thuc, E. Hossain and H. Tabassum, "Downlink Power Control in Two-Tier Cellular Networks With Energy-Harvesting Small Cells as Stochastic Games," in IEEE Transactions on Communications, vol. 63, no. 12, pp. 5267-5282, Dec. 2015.

[36] D. Qin, W. Xu and Z. Ding, "Power control and resource allocation for capacity improvement in picocell downlinks," 2012 International Conference on Wireless Communications and Signal Processing (WCSP), Huangshan, 2012, pp. 1-6.

[37] C. Vlachos and V. Friderikos, "MOCA: Multiobjective Cell Association for Device-to-Device Communications," in IEEE Transactions on Vehicular Technology, vol. 66, no. 10, pp. 9313-9327, Oct. 2017.

[38] Y. Chen, S. Zhang, S. Xu, and G. Y. Li, "Fundamental tradeoffs on green wireless network," IEEE Commun. Mag., vol. 49, no. 6, pp. 30-37, Jun. 2011.

[39] C. Bae and W. Stark, "Energy-bandwidth tradeoff with spatial reuse in wireless multi-hop networks," in Proc. IEEE MILCOM Conf., San Diego, CA, USA, Nov. 16-19, 2008, pp. 1-7.

[40] A. Chockalingam and M. Zorzi, "Energy efficiency of media access protocols for mobile data networks," in IEEE Transactions on Communications, vol. 46, no. 11, pp. 1418-1421, Nov 1998.

[41] Shahab, Suhail Najm and Abdulkafi, Ayad Atiyah and Ayib Rosdi, Zainun (2015) "Assessment of Area Energy Efficiency of LTE Macro Base Stations in Different Environments," Journal of Telecommunications and Information Technology, 1 . pp. 59-66. ISSN 1509-4553.

[42] C. Xiong, G. Y. Li, S. Zhang, Y. Chen and S. Xu, "Energy- and Spectral-Efficiency Tradeoff in Downlink OFDMA Networks," in IEEE Transactions on Wireless Communications, vol. 10, no. 11, pp. 3874-3886, November 2011.

[43] H. Mahdavi-Doost, N. Prasad and S. Rangarajan, "Optimizing Energy Efficiency Over Energy-Harvesting LTE Cellular Networks," in IEEE Transactions on Green Communications and Networking, vol. 1, no. 3, pp. 320-332, Sept. 2017.

[44] R. Mahapatra, Y. Nijsure, G. Kaddoum, N. Ul Hassan and C. Yuen, "Energy Efficiency Tradeoff Mechanism Towards Wireless Green Communication: A Survey," in IEEE Communications Surveys and Tutorials, vol. 18, no. 1, pp. 686-705, Firstquarter 2016.

[45] K. Pawlikowski, H. -. J. Jeong and J. -. R. Lee, "On credibility of simulation studies of telecommunication networks," in IEEE Communications Magazine, vol. 40, no. 1, pp. 132-139, Jan. 2002.

[46] N. I. Sarkar and J. A. Gutierrez, "Revisiting the issue of the credibility of simulation studies in telecommunication networks: highlighting the results of a comprehensive survey of IEEE publications," in IEEE Communications Magazine, vol. 52, no. 5, pp. 218-224, May 2014.

[47] Michael Neely, "Stochastic Network Optimization with Application to Communication and Queueing Systems," in Stochastic Network Optimization with Application to Communication and Queueing Systems, Morgan & Claypool, 2010, pp.